**Splitting a C-O bond in dialkylethers with bis(1,2,4-tri-t-butylcyclopentadienyl) cerium-hydride does not occur by a σ-bond metathesis pathway: a combined experimental and DFT computational study.**

Evan L.Werkema,[a] Ahmed Yahia,[b,c] Laurent Maron,[b] Odile Eisenstein[d] and Richard A. Andersen[a].

a) Department of Chemistry and Chemical Sciences Division of Lawrence Berkeley National Laboratory, University of California, Berkeley, California 94720-1460. b) LPCNO, Université de Toulouse, INSA, UPS, LPCNO, 135 avenue de Rangueil, F-31077 Toulouse, France, and CNRS, LPCNO, F-31077 Toulouse, France, c) ICSM UM5257, CEA-CNRS-UM2, Site de Marcoule, BP17171, 30207 Bagnols-sur-Cèze, France, d) Institut Charles Gerhardt, Université Montpellier 2, CNRS 5253, cc 1501, Place E. Bataillon, F-34095 Montpellier France.

This work was supported by the Director, Office of Science, Office of Basic Energy Sciences, of the U.S. Department of Energy under Contract No. DE-AC02-05CH11231.

This work was supported by the Assistant Secretary for Energy Efficiency and Renewable Energy, Office of Building Technology, State, and Community Programs, of the U.S. Department of Energy under Contract No. DE-AC02-05CH11231.

**DISCLAIMER**

**Abstract**

Addition of diethylether to $[1,2,4(Me_3C)_3C_5H_2]_2CeH$, abbreviated $Cp'_2CeH$, gives $Cp'_2CeOEt$ and ethane. Similarly, di-n-propyl- or di-n-butylether gives $Cp'_2Ce$(O-n-Pr) and propane or $Cp'_2Ce$(O-n-Bu) and butane, respectively. Using $Cp'_2CeD$, the propane and butane contain deuterium predominantly in their methyl groups. Mechanisms, formulated on the basis of DFT computational studies, show that the reactions begin by an α- or β-CH activation with comparable activation barriers but only the β-CH activation intermediate evolves into the alkoxide product and an olefin. The olefin then inserts into the Ce-H bond forming the alkyl derivative, $Cp'_2CeR$, that eliminates alkane. The α-CH activation intermediate is in equilibrium with the starting reagents, $Cp'_2CeH$ and the ether, which accounts for the deuterium label in the methyl groups of the alkane. The one-step σ-bond metathesis mechanism has a much higher activation barrier than either of the two-step mechanisms.

**Introduction**

It has been shown recently that the monomeric metallocenecerium hydride $[1,2,4(Me_3C)_3C_5H_2]_2CeH$, $Cp'_2CeH$, (shown in Scheme 1) reacts with methyl halides forming the seemingly straightforward H for X exchange products, $Cp'_2CeX$ and methane, eq. 1.

$$Cp'_2CeH + CH_3X \longrightarrow Cp'_2CeX + CH_4 \qquad (1)$$

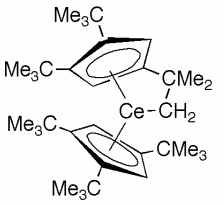


$Cp'[(Me_3C)_2C_5H_2C(CH_3)_2CH_2]Ce$

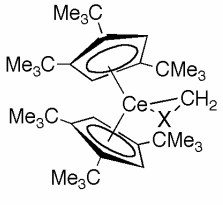


$Cp'_2Ce(\eta^2\text{-}CH_2X)$

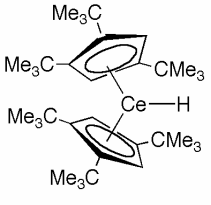


$Cp'_2CeH$

**Scheme 1**

The mechanism of the exchange reaction does not proceed by way of a direct σ-bond metathesis transition state, since experimental and computational studies showed that the reactions proceed by a two-step mechanism forming the products shown in eq. 1. The first step is a CH bond activation generating a carbenoid intermediate, $Cp'_2Ce(\eta^2\text{-}CH_2X)$, and $H_2$ followed by a second step that involves trapping of $CH_2$ by $H_2$.[1,2] No intermediates were observed in the reactions of $Cp'_2CeH$ by NMR spectroscopy. When the metallacycle $Cp'[(Me_3C)_2C_5H_2C(CH_3)_2CH_2]Ce$ (shown in Scheme 1) is used, i.e., when $H_2$ is not present, NMR evidence was obtained for an intermediate, $Cp'_2Ce(\eta^2\text{-}CH_2X)$ (shown in Scheme 1) when X = Cl, Br, I, eq. 2.

$$Cp'[(Me_3C)_2C_5H_2C(CH_3)_2CH_2]Ce + CH_3X \longrightarrow Cp'_2Ce(\eta^2\text{-}CH_2X) \longrightarrow Cp'_2CeX + \text{“}CH_2\text{”} \qquad (2)$$

When X = OMe, $Cp'_2Ce(\eta^2\text{-}CH_2OMe)$ was isolated, even in presence of $H_2$ and the methoxymethyl derivative slowly formed $Cp'_2CeOMe$.[2] The net reaction of $Me_2O$ with $Cp'_2CeH$ that gives $Cp'_2CeOMe$ and $CH_4$ is analogous to the net reaction between $(C_5Me_5)_2MH$ and $Et_2O$, which gives the ethoxide, $(C_5Me_5)_2MOEt$, and ethane. The reaction was first reported by Watson[3] for M = Lu, who showed that when $Et_2O\text{-}d_{10}$ was used, the ethane isotopologue is $CHD_2CD_3$ and no ethene was observed. This result lead to the suggestion that ethane was formed by direct attack of the hydride on the carbon α to the oxygen. This statement clearly implicates a four-center mechanism for the reaction, although the term σ-bond metathesis, coined by

Bercaw and co-workers, was not in the literature at the time of Watson's initial studies.[4] The mechanism of a σ-bond metathesis reaction, *i.e.*, a net reaction in which the σ bonds exchange partners, is a concerted process that occurs in a single step in which the four participating atoms or groups has a kite-shaped transition state. In this article, the term σ -bond metathesis transition state and mechanism of a σ -bond metathesis reaction refer to the same physical mechanism or pathway. Later, the σ-bond metathesis terminology was used by Teuben and co-workers to describe the analogous reactions between $(C_5Me_5)_2MH$, M = Y, La, Ce and $Et_2O$.[5] A similar pathway was mentioned for the formation of $(C_5Me_5)_2SmOEt$ from $(C_5Me_5)_2SmH$ and $Et_2O$.[6]

Computational studies on the reaction between $(C_5H_5)_2CeH$ and $Me_2O$ showed that the activation barrier for a σ-bond metathesis transition state is higher than that of the two-step pathway by about 4 kcal $mol^{-1}$; a deduction that is consistent with the experimental studies on $Cp'_2CeH$.[2] Thus, a mechanistic quandary is apparent since if the σ-bond metathesis transition state is a high energy pathway for $Me_2O$, then it is presumably also high for $Et_2O$. If this conjecture is correct, then the mechanism for the formation of $Cp_2CeOEt$ and ethane could proceed by either i) σ-bond metathesis ii) α- or perhaps by iii) β-CH activation where the α and β CH notation refers to the CH bonds α or β to the oxygen atom of the ether, respectively.

In this article, we show that the reaction between $Cp'_2CeH$ and the symmetrical dialkylethers $RCH_2CH_2OR'$ (R = H, Me, Et; R' = $CH_2CH_2R$) does not proceed by way of the single step σ-bond metathesis transition state but by way of a two-step process, the first of which is a β-CH activation followed by an alkoxy transfer step with olefin elimination. In a subsequent reaction, the olefin inserts into the Ce-H

bond forming an alkyl complex that reacts with $H_2$ forming an alkane and $Cp'_2CeH$ or alkane elimination forming the metallacycle and alkane. Thus the net C-O bond cleavage reaction is as shown in eq. 3.

$$Cp'_2CeH + RCH_2CH_2OR' \longrightarrow Cp'_2CeOR' + CH_3CH_2R \qquad (3)$$

**Results**

*1) Experimental Studies*

The reactions between $Cp'_2CeH$ and the dialkyl ethers are conducted in NMR tubes and the course of the reaction is monitored by $^1H$ NMR spectroscopy. The reactions are slow as shown by the disappearance of the resonances due to $Cp'_2CeH$ and appearance of the resonances due to $Cp'_2CeOR'$ and $CH_3CH_2R$, eq. 3. For example, the ratio of $Cp'_2CeH$ to $Cp'_2CeOEt$ is approximately 1:4 after 36 days at 20° C. The ratio of $Cp'_2CeH$ to $Cp'_2CeO$-n-Pr or $Cp'_2CeO$-n-Bu is approximately 1:2 after 101 days at 60° C and the relative rates are Et >> n-Pr ≈ n-Bu. The alkoxide derivatives are isolated and characterized as outlined in the Experimental section. In contrast, the reaction between $Cp'_2CeH$ and $Me_2O$ rapidly forms $Cp'_2Ce(\eta^2$-$CH_2OMe)$ and $H_2$, and the former slowly evolves into the methoxide, $Cp'_2CeOMe$.[2] When R' is Et, n-Pr and n-Bu, no resonances due to a hypothetical α-CH activation intermediate $Cp'_2Ce(C(H)(CH_2R)OR')$ are detected, which implies that if α-CH activation occurs, the intermediates go straight to the alkoxide products, or the net reactions follow a different pathway such as β-CH activation or direct elimination of $CH_3CH_2R$.

An experimental distinction between a direct alkane elimination or an α- or β-CH activation preceeding alkane formation is possible using deuterium labeled $(Cp'\text{-}d_{27})_2CeD$ and n-$Pr_2O$ or n-$Bu_2O$, since these reactions are clean, but slow and the deuteria incorporated into the various sites of the ethers and hydrocarbon can be monitored over time. For example, monitoring the reaction between $(Cp'\text{-}d_{27})_2CeD$ and n-$Bu_2O$ in $C_6D_6$ by $^1H$, $^2H$, and $^{13}C\{^1H\}$ NMR spectroscopy shows that deuterons are incorporated into the α, and δ-sites in non-statistical amounts. After 147 days at 60° C, when the conversion of $(Cp'\text{-}d_{27})_2CeD$ to $(Cp'\text{-}d_{27})_2CeO\text{-}n\text{-}Bu$ is complete, the relative distribution of deuterons into the excess $(n\text{-}Bu)_2O$ is α >> δ in the $^2H$ and $^{13}C\{^1H\}$ NMR spectra. Using the integrated intensities of the two resonances in the $^2H$ NMR spectrum yields the α:δ ratio of 10:1. This result shows that H/D exchange accumulates deuterons into the α-site, which implies that α-CH activation is reversible. No deuterium is detected in the β or γ-sites of $(n\text{-}Bu)_2O$, but the butane produced by the reaction contains deuterium in both the primary and secondary sites in a ratio of 5:1. This result implies that β-CH activation is productive in splitting the C-O bond to generate the alkoxide and a terminal alkene, which is hydrogenated to the alkane by $Cp'_2CeH$. A similar conclusion is reached from an analysis of the reaction between $(Cp'\text{-}d_{27})_2CeD$ and n-$Pr_2O$; see Experimental Section for details. These studies show that the mechanism for ether cleavage depends upon whether the ethers have β-hydrogens. The different reaction mechanisms are explored by computational studies outlined in the following section.

*2) Computational studies*

The DFT(B3PW91) calculations utilized the methodology described in previous studies.[1,2,7] As before, Cp' is modeled by Cp ($C_5H_5$) due to the prohibitive of

calculations involving the full Cp' metallocenes. While a substitution alters the geometric and steric environment of the metal center, and consequently the absolute values of the calculated energies, the reactivity trends predicted computationally for Cp complexes for small molecules generally agree with those observed experimentally for the analogous Cp' complexes. The modeling should likewise be valid for the ether reactions presented in this paper

The free energy profiles for the reaction of $Cp_2CeH$, abbreviated as [Ce]H with $Et_2O$, n-$Pr_2O$, and n-$Bu_2O$ are shown in Fig. 1. The Gibbs free energy, G, of all extrema are given relative to the separated reactants [Ce]H and ether. The activation barrier is defined as the difference in Gibbs free energy between a transition state and its associated reactant.

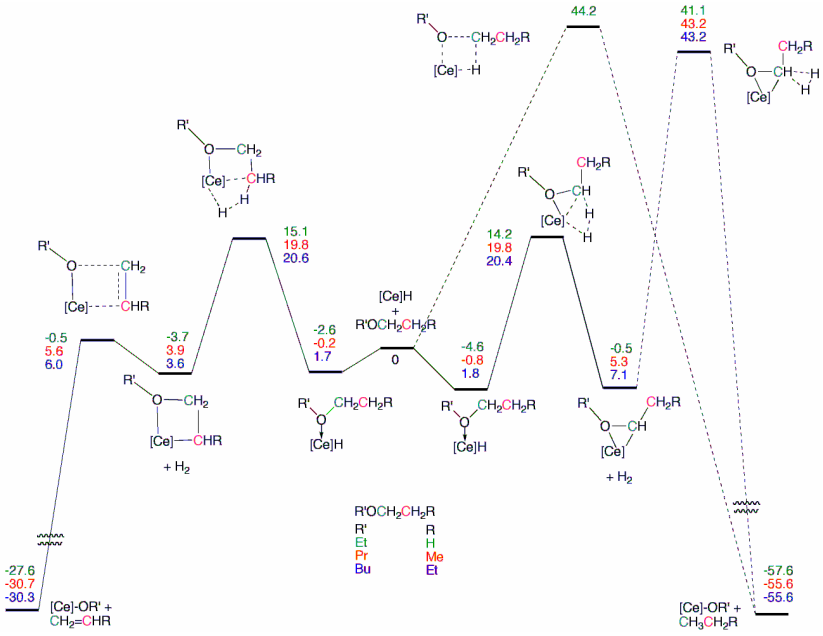

**Fig 1.** Free energy profiles (kcal $mol^{-1}$) for the reaction pathways of [Ce]H with $Et_2O$, n-$Pr_2O$ and n-$Bu_2O$. On the right, the σ-bond metathesis and the α-CH activation. On the left, β-CH activation.

The one-step σ-bond metathesis reaction is calculated for $Et_2O$. The transition state has a Gibbs free energy of 44.2 kcal $mol^{-1}$. This is close to 43.5 kcal $mol^{-1}$ value obtained for $Me_2O$, and higher than those obtained for $CH_3X$ when X equals halide.[2] These two values strongly indicate that the direct H for OR exchange is not the mechanism for the formation of [Ce]OEt. This path was not explored for n-$Pr_2O$ and n-$Bu_2O$ reactions. The alternative mechanistic pathways are explored next.

The α-CH activation starts by the formation of an ether adduct whose free energy of -4.6 kcal $mol^{-1}$ slightly beats the loss in entropy and formation of the adducts is exoergic. The transition state for the α-CH bond activation has a free energy of 14.2 kcal $mol^{-1}$ relative to separated [Ce]H and ether, very close to the value of 13.8 kcal $mol^{-1}$ obtained for $Me_2O$. The resulting 3-member ring [Ce]($\eta^2$-$CH(CH_3)OEt$) has a Gibbs free energy of -0.5 kcal $mol^{-1}$, essentially equal to that of -0.9 for [Ce]($\eta^2$-$CH_2$-OMe). From this intermediate, the free energy of the transition state for insertion of $CH(CH_3)$ into $H_2$ is 41.1 kcal $mol^{-1}$, slightly higher than that of 37.9 kcal $mol^{-1}$ calculated for [Ce]($\eta^2$-$CH_2OMe$). The trapping reaction of $CH_2$ by $H_2$ was shown previously, in the case of [Ce]($\eta^2$-$CH_2F$), [Ce]($\eta^2$-$CHF_2$) and [Ce]($\eta^2$-$CF_3$) with $H_2$, to be largely controlled by the electrophilicity of the carbene that is formed on cleavage of the C-F and Ce-C bond.[1] A similar effect is apparent in this case even though the π-electron donating ability of the methyl group in CH(Me) is less than that of F. The high activation barrier of the trapping reaction means that the α-CH activation pathway is not productive. Since the activation barrier for the α-CH activation step is

low and since the ether adduct and the [Ce]($\eta^2$-CH(Me)OEt) intermediate are isoergic, an equilibrium exists between these two molecules, which accounts for accumulation of the deuterium in the α-sites of the dialkylethers.

The β-CH activation pathway starts from an adduct at -2.6 kcal $mol^{-1}$, similar to that for the α-CH activation; the adducts differ only in the conformation of the two Et groups. From this adduct, the transition state for β-CH activation has a Gibbs free energy of 15.1 kcal $mol^{-1}$, only slightly higher than that for the α-CH activation. From this transition state, the four-member CeOCC ring with an energy of -3.7 kcal $mol^{-1}$ is slightly more stable than the three-member CeOC ring originating from the α-CH activation, reflecting the decreased ring strain in the four-member ring. The four-membered ring metallacycle [Ce]($\eta^2$-$CH_2$-$CH_2$-OEt), evolves into the products, $CH_2$=$CH_2$ and [Ce]OEt, with a low activation energy of -3.2 kcal $mol^{-1}$ . The favorable free energy of reaction of -27.6 kcal $mol^{-1}$ is the result of the formation of a strong Ce-OR bond.

[Ce]OEt is an observed product but ethene is not since only the saturated alkane, ethane in this case, is observed. Several pathways are possible for the conversion of ethylene to ethane; i) ethylene can insert into the Ce-H bond and the resulting [Ce]Et undergoes hydrogenolysis with $H_2$ forming [Ce]H and ethane, or ii) the ethyl complex can eliminate ethane forming the metallacycle since the isolated Cp'$_2$Ce$CH_2$Ph reacts with $H_2$ to form Cp'$_2$CeH and toluene, and forms the metallacycle and toluene in absence of $H_2$, both pathways are reasonable ones for formation of alkane from the hypothetical alkyl, Cp'$_2$Ce$CH_2CH_2$R.[8] Insertion of an olefin into a metal hydride bond for the $d^0$ metal complexes has been extensively studied by computations as the initial step in polymerization reactions;[9] in all cases the activation barrier is low, which

accounts for the fact that no transition state for ethylene insertion in the Ce-H bond was located. Given the large body of computational studies that show the low activation barriers for olefin insertion, the formation of an alkane product was not explored computationally for $Cp_2CeH$ and an olefin in this article.

The structures of the intermediates and transition states for these two reactions are not surprising (Figs. 2 and 3). The geometry for the α-CH activation with $Et_2O$ is similar to that for $Me_2O$, the main characteristic being the open $C_\alpha{\cdots}H{\cdots}H$ angle of 171°. The geometry for the β-CH activation has the same angle $C_\beta{\cdots}H{\cdots}H$ of 171° (Fig. 2). The slightly higher energy of the transition state for β-CH activation compared to that of α-CH activation is, in part, due to the eclipsed orientation of the ethyl group in the transition state.

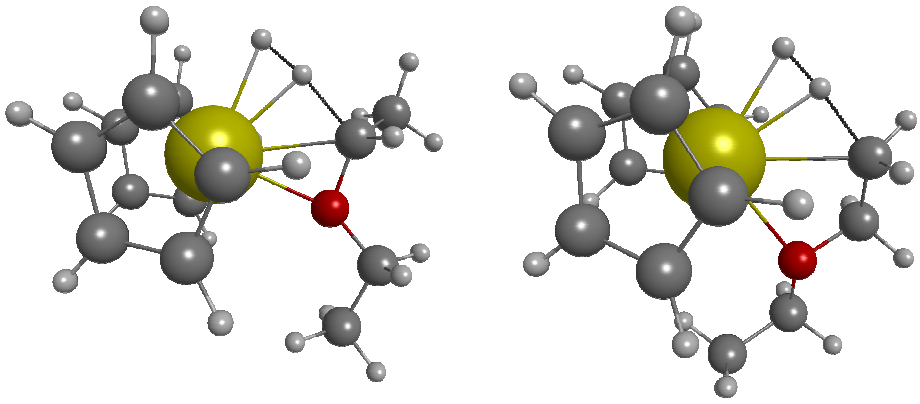

**Fig. 2** Optimized structures of the transition states for, left, the α-C-H activation and, right, the β-CH activation. The color codes are yellow for cerium, red for oxygen, dark grey for carbon, light grey for hydrogen.

The three-membered CeOC ring in [Ce]($\eta^2$-CHMeOEt) has similar features (Ce-C = 2.552 Å; Ce-O = 2.450 ; C-O= 1.464 Å to those calculated for [Ce]( $\eta^2$-$CH_2OMe$) (Ce-C = 2.510 Å, Ce-O = 2.445 Å; C-O = 1.461 Å ).[2] The marginal lengthening of the Ce-C bond in [Ce]($\eta^2$-CHMeOEt) is due to the steric effect of the ethyl substituent. The four-membered CeOCC ring resulting from β-CH activation is planar (Fig. 3). The C-C bond length of 1.51 Å is close to the value for C-C single bond (1.54 Å) and the Ce-C bond of 2.58 Å, is identical to that of 2.577(4) Å, observed in $Cp'_2CeCH_2Ph$,[8] and an elongated intra-ring C-O distance of 1.45 Å, compared to the exo-ring C-O(Et) distance of 1.42Å. The calculated Ce-O bond length is 2.529 Å. Comparison with an experimental value is not available since only the structure of the three-membered ring [Ce]($\eta^2$-$CH_2OMe$) is known. The transition state for ethene elimination shows an elongation of the "long" C-O bond to a distance of 1.775 Å, stretching the Ce-C bond to 2.653 Å, while shortening the C-C distance to 1.424 Å, and also of the Ce-O bond to 2.378 Å as it forms the Ce-O bond of 2.163 Å in [Ce]OEt (Fig. 3). The four-membered ring remains planar at the transition state and the ethylene is essentially planar, since the angles at carbon sum to 348.5°.

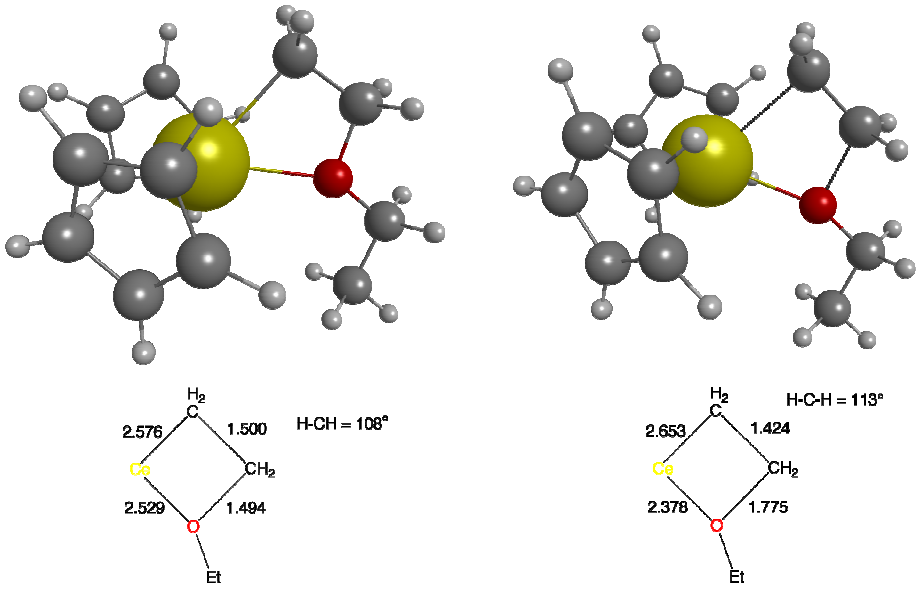


**Fig. 3** Optimized structures for (a) the four-membered ring [Ce]($\eta^2$-CHRCH$_2$OR') (R = H, R' = CH$_2$CHR) and (b) the associated transition states for the ejection of CHR=CH$_2$. The geometrical features are similar for R = Me and Et. The selected distances are in Å and angles in degrees. The color codes are yellow for cerium, red for oxygen, dark grey for carbon and light grey for hydrogen.

The reaction pathways for the reactions of n-Pr$_2$O and n-Bu$_2$O with [Ce]H are similar to those obtained for Et$_2$O, but all intermediates and transition states are higher in energy by 5 to 7 kcal mol$^{-1}$ relative Et$_2$O. Since the free energy profiles for n-Pr$_2$O and n-Bu$_2$O are close together, the substituents closer to the oxygen atom have a larger influence on the energies than those further away and the relative free energy profiles are in good agreement with the relative rates observed as one proceeds from Et$_2$O to n-Pr$_2$O to n-Bu$_2$O in the experimental reaction.

**Discussion**

The net reaction between $Cp'_2CeH$ and dialkyl ethers results in the alkoxy for H exchange illustrated in eq. 3. Computational studies show that of the three possible mechanisms considered, the direct exchange through a σ-bond metathesis transition state has the highest activation barrier. Lower energy processes that involve the initial α- or β-CH activation forming three and four-membered ring intermediates, respectively, are comparable in energy. These relative energies should not be significantly changed with Cp' ligands instead of Cp, and in particular the σ-bond metathesis pathway should remain the pathway with the highest energy barrier. The essentially equivalent activation barriers for α- and β-CH activation show that the acidity of the CH bonds is not the only factor that determines the selectivity, but the ring strain at the transition state is also important. These intermediates evolve into product by ejection of a carbene or an olefin, respectively, and the activation barrier for the former is substantially higher than that for the latter transformation. Thus, the α-CH activation intermediate does not lead to product whereas the β-CH activation intermediate leads to the C-O bond cleavage. The relative activation barriers identified in the computational studies of the potential energy surfaces for the three pathways considered are consistent with the experimental observations that show i) the rates of the reactions are slow, ii) deuterium from $Cp'_2CeD$ is preferentially distributed into the α-CH sites of the dialkylethers and the terminal methyl groups in the alkanes, and iii) no intermediates build up in sufficient concentration to be detected by $^1H$ NMR spectroscopy. The eliminated olefin is postulated to be trapped by $Cp'_2CeH$ forming the alkyl that rapidly undergoes hydrogenolysis or/and alkane elimination forming the metallacycle, which is trapped by $H_2$ reforming $Cp'_2CeH$. The principle that emerges from these studies is that even though an alkane rather than an olefin is the product observed when the ether contains β-hydrogens, the

reaction proceeds by way of olefin elimination and the olefin is converted to the alkane rapidly. This accounts for the lack of detectable intermediates, in contrast to, for example, the isolation of $Cp'_2Ce(\eta^2\text{-}CH_2OMe)$ when $Me_2O$ is used.[2] Thus, the C-O cleavage reaction in dialkylethers leads to the net alkoxy for hydrogen exchange, and the mechanism depends upon the nature of the alkyl group.

The reactions of $Cp'_2CeH$ with dialkylethers described in this and an earlier article[2] have a parallel with reactions of alkyllithium reagents with $Me_2O$ and $Et_2O$. Ziegler showed, sixty years ago, that $Me_2O$ and RLi generate a "methylene carbenoid" that evolves into LiOMe and $LiCH_2R$.[10] Thus, the organolithium reagent traps the methylene fragment, a net reaction that is somewhat similar to the reaction of $Cp'_2CeH$ and $Me_2O$.[2] Later it was shown that RLi reagents react with appropriately labeled diethylether to give lithium alkoxides and an olefin; the distribution of deuterium shows that the major pathway is β-CH abstraction, though a small fraction is formed by α-C-H abstraction, similar to the reactions described in this article.[11] The ether cleavage reactions have considerable synthetic utility and are the subject of reviews.[12]

The choice between α- and β-CH activation pathways in ethers carries over to amines. The metalation reaction of $Me_2NCH_2CH_2NMe_2$ with $LiCMe_3$ gives $Me_2NCH_2CH_2N(Me)(CH_2Li)$ and $Me_3CH$ but, with $Et_2NCH_2CH_2NEt_2$ the products are $Et_2NCH_2CH_2N(Et)(Li)$, ethylene and $Me_3CH$.[13] Computational studies outlined in this article also show that the β-CH activation energy is about 5 kcal $mol^{-1}$ lower than that for α-CH activation. In d-transition metal chemistry, addition of, for example, diethylether to a zirconium metallocene gives [Zr](H)(OEt) and $[Zr](C_2H_4)$ where [Zr] is a bis(substituted indenyl) metallocene fragment. The suggested mechanism

involves an equilibrium between the α- and β-CH activation intermediates and the latter evolves into the two isolated products.[14] It is noteworthy that the four-membered ring, $MOCH_2CH_2$ intermediate advocated in this article may be important in the exchange of β-CH's with deuterons in $Ta(OEt)_5$ and EtOD and related alcohols.[15]

## Conclusion

The experimental reaction between $Cp'_2CeH$ and the dialkylether $RCH_2CH_2OR'$, where R = H, Me, Et; R' = $CH_2CH_2R$) gives $Cp'_2CeOR'$ and R'H. The DFT calculations of the potential energy surfaces for each ether with $(C_5H_5)_2CeH$ shows that a one-step OR' for H exchange pathway has a higher activation barrier than two different two-step pathways that begin by α- or β-CH activation forming $Cp_2Ce[\eta^2$-$CH(CH_2R)OR']$ and $Cp_2Ce[\eta^2$-$CH(R)CH_2OR']$, respectively, both of which have comparable activation barriers, but only the latter intermediate yields the alkoxide product with evolution of an olefin. The mechanistic pattern that emerges from the combined experimental and computational studies is that β-CH activation followed by olefin elimination has a lower activation barrier than α-CH activation followed by carbene elimination. This reactivity pattern seems to be general for metals that cannot undergo oxidative addition-reductive elimination cycles.

## Experimental Section

### General

All manipulations were performed under an inert atmosphere using standard Schlenk and dry box techniques. All solvents and ethers were dried and distilled from sodium or sodium benzophenone ketyl. Alkoxytrimethylsilane reagents were distilled under nitrogen and vacuum transferred into greaseless flasks. NMR spectra were

recorded on Bruker AV-300, AV-400, or AV-600 spectrometers at 20°C in the solvent specified. J-Young NMR tubes or sealed NMR tubes were used for all NMR tube experiments. Electron impact mass spectrometry and elemental analyses were performed by the microanalytical facility at the University of California, Berkeley. The abbreviation Cp' is used for the 1,2,4-tri-*tert*-butylcyclopentadienyl ligand. GCMS analysis was performed on an HP6890 GC system with a J&W DB-XLB universal non-polar column, attached to an HP5973 Mass Selective Detector.

**Syntheses**

**Cp'$_2$CeOEt.**

Cp'$_2$CeH[16] (0.55g, 0.90 mmol) was dissolved in pentane (10 mL) and ethoxytrimethylsilane (0.2 mL, 1.3 mmol) was added via syringe. The purple solution turned red over 10 minutes. After 30 minutes, the sample was taken to dryness and the glassy red solid was added to glass ampoules, sealed under vacuum, and sublimed at 185°C. The resulting deep red plates and microcrystals were sealed under vacuum in a fresh ampoule and sublimed again at 185°C. Yield: 150 mg (0.23 mmol, 25%). MP = 317-319°C. $^1$H NMR ($C_6D_6$): δ 32.88 (2H, $\nu_{1/2}$ = 30 Hz), 24.40 (4H, $\nu_{1/2}$ = 60 Hz), 11.06 (3H, $\nu_{1/2}$ = 15 Hz), -1.69 (36H, $\nu_{1/2}$ = 40 Hz), -11.11 (18H, $\nu_{1/2}$ = 25 Hz). MS $(M)^+$ *m/z* (calc, found) 651 (100, 100) 652 (40, 53) 653 (20, 32) 654 (6, 15) 655 (1, 3). Anal. Calcd. for $C_{36}H_{63}CeO$: C, 66.32; H, 9.74. Found C, 66.29; H, 9.64.

**Cp'$_2$CeO-n-Pr.**

Cp'$_2$CeH (0.42g, 0.69 mmol) was dissolved in pentane (10 mL) and n-propoxytrimethylsilane (0.15 mL, 0.87 mmol) was added via syringe. The purple solution turned red over 10 minutes. After 30 minutes, the sample was taken to dryness and the glassy red solid was added to glass ampoules, sealed under vacuum,

and sublimed at 185°C. The resulting deep red microcrystals were sealed under vacuum in a fresh ampoule and sublimed again at 185°C. Yield: 130 mg (0.19 mmol, 28%). MP = 315-318°C. $^1$H NMR ($C_6D_6$): δ 33.25 (2H, $\nu_{1/2}$ = 30 Hz), 24.74 (4H, $\nu_{1/2}$ = 70 Hz), 11.66 (2H, $\nu_{1/2}$ = 15 Hz), 5.85 (3H, $\nu_{1/2}$ = 15 Hz), -1.48 (36H, $\nu_{1/2}$ = 80 Hz), -11.73 (18H, $\nu_{1/2}$ = 25 Hz). MS $(M)^+$ *m/z* (calc, found) 665 (100, 100) 666 (41, 52) 667 (21, 30) 668 (6, 7). Anal. Calcd. for $C_{37}H_{65}CeO$: C, 66.72; H, 9.84. Found C, 66.89; H, 10.12.

**Cp'$_2$CeO-n-Bu.**

n-Butoxytrimethylsilane was prepared from n-butyl alcohol, chlorotrimethylsilane, and triethylamine following published procedures.[17] Cp'$_2$CeH (0.38g, 0.63 mmol) was dissolved in pentane (10 mL) and n-butoxytrimethylsilane (0.16 mL, 0.85 mmol) was added via syringe. The purple solution turned red over 10 minutes. After 30 minutes, the sample was taken to dryness, warmed gently under dynamic vacuum to remove excess n-butoxytrimethylsilane, and the glassy red solid was added to glass ampoules, sealed under vacuum, and sublimed at 185°C. The resulting gummy, deep red solid was sealed under vacuum in a fresh ampoule and sublimed again at 185°C. Yield: 60 mg (0.088 mmol, 14%). $^1$H NMR ($C_6D_6$): δ 33.43 (2H, $\nu_{1/2}$ = 40 Hz), 24.75 (4H, $\nu_{1/2}$ = 70 Hz), 11.71 (2H, $\nu_{1/2}$ = 25 Hz), 6.63 (2H, $\nu_{1/2}$ = 25 Hz), 3.62 (3H, t, *J* = 8 Hz), -1.40 (36H, $\nu_{1/2}$ = 85 Hz), -11.80 (18H, $\nu_{1/2}$ = 30 Hz). MS $(M)^+$ *m/z* (calc, found) 679 (100, 100) 680 (42, 56) 681 (21, 35) 682 (6, 15). Anal. Calcd. for $C_{37}H_{65}CeO$: C, 67.11; H, 9.93. Found C, 67.28; H, 10.11.

**NMR Tube Reactions**

**Cp'$_2$CeH and ethoxytrimethylsilane in benzene-d$_6$.**

Cp'$_2$CeH was dissolved in $C_6D_6$ in an NMR tube and a drop of ethoxytrimethylsilane was added. The sample turned red over 2 minutes, by which

time resonances due to $Cp'_2CeH$ had disappeared from the $^1H$ NMR spectrum, and resonances due to trimethylsilane[18] and $Cp'_2CeOEt$ had appeared. Integration of the $CMe_3$ resonances relative to the solvent residual proton signal indicated that the conversion from $Cp'_2CeH$ was quantitative.

**$Cp'_2CeH$ and propoxytrimethylsilane in benzene-$d_6$.**

$Cp'_2CeH$ was dissolved in $C_6D_6$ in an NMR tube and a drop of n-proxytrimethylsilane was added. The sample turned red over 2 minutes, by which time resonances due to $Cp'_2CeH$ had disappeared from the $^1H$ NMR spectrum, and resonances due to trimethylsilane and $Cp'_2CeO$-n-Pr had appeared. Integration of the $CMe_3$ resonances relative to the solvent residual proton signal indicated that the conversion from $Cp'_2CeH$ was quantitative.

**$Cp'_2CeH$ and diethyl ether ($Et_2O$) in cyclohexane-$d_{12}$.**

$Cp'_2CeH$ was dissolved in $C_6D_{12}$ in an NMR tube and a drop of $Et_2O$ was added. The sample was allowed to stand at 19°C. After 1 day, a new set of paramagnetic resonances due to $Cp'_2CeOEt$ had appeared in the $^1H$ NMR spectrum; the ratio of $Cp'_2CeH$ to $Cp'_2CeOEt$ was 30:1. After 9 days, the ratio was 2:1; after 36 days, 1:4; and after 52 days, 1:20.

**$Cp'_2CeH$ and dipropyl ether (n-$Pr_2O$) in cyclohexane-$d_{12}$.**

$Cp'_2CeH$ was dissolved in $C_6D_{12}$ in an NMR tube and a drop of n-$Pr_2O$ was added. The sample was heated at 60°C. After 1 day, resonances due to $Cp'_2CeO$-n-Pr had appeared in the $^1H$ NMR spectrum; the ratio of $Cp'_2CeH$ to $Cp'_2CeO$-n-Pr was 33:1. After 16 days, the ratio was 5:1; after 54 days, 1.2:1; after 101 days, 1:2; and after 186 days, 1:10.

**$(Cp'\text{-}d_{27})_2CeD$ and n-$Pr_2O$ in $C_6D_6$.**

Cp'$_2$CeH was dissolved in $C_6D_6$ and heated at 60°C for 4 days to perdeuterate the $CMe_3$ groups. The sample was taken to dryness and the solid residue was dissolved in fresh $C_6D_6$. The sample was heated for an additional 4 days, then taken to dryness, and the solid residue was dissolved in $C_6D_6$. The $^2$H NMR spectrum contained $C(CD_3)_3$ resonances consistent with (Cp'-$d_{27}$)$_2$CeD. A drop of n-$Pr_2O$ was added, and the sample was heated at 60°C. After 1 day, a broad resonance at 3.14 ppm had appeared in the $^2$H NMR spectrum, and a 1:1:1 pattern centered at 72.52 ppm ($J_{CD}$ = 21 Hz) had appeared in the $^{13}$C NMR spectrum 0.4 ppm upfield of the signal for the α-carbons of n-$Pr_2O$, indicating H-for-D exchange. After 16 days, resonances due to (Cp'-$d_{27}$)$_2$CeOPr had appeared in the $^2$H NMR spectrum; the ratio of (Cp'-$d_{27}$)$_2$CeD to (Cp'-$d_{27}$)$_2$CeOPr was 12:1. The spectrum also contained a triplet at 3.14 ($J_{HD}$ = 1 Hz) and a multiplet at 0.82 ppm, indicating H-for-D exchange had occurred on the α- and γ-carbons of n-$Pr_2O$; the area ratio of the resonances was 14:1. The triplet in the $^1$H NMR spectrum due to protons on the α-carbons of n-$Pr_2O$ had shifted upfield by 0.02 ppm, and each peak was split into a 1:1:1 pattern ($J_{HH}$ = 7 Hz, $J_{HD}$ = 1 Hz). The resonance for the protons on the β-carbons had changed from a coincidental sextet (triplet of quartets) to a quartet ($J_{HH}$ = 7 Hz), and the area ratio of the proton resonances for the α-, β-, and γ-carbons was 1:19:27. A triplet with each peak split into a 1:1:1 pattern due to γ-$CH_2D$ groups in n-$Pr_2O$ had appeared 0.017 ppm upfield of the triplet corresponding to γ-$CH_3$ groups. The $^{13}$C NMR spectrum contained a multiplet at 72.03 ppm ($J_{CD}$ = 21 Hz) for the α-carbons, a singlet for the β-carbons, and a singlet plus a 1:1:1 pattern ($J_{CD}$ = 19 Hz) centered 0.29 ppm upfield of the singlet for the γ-carbon resonance. After 186 days, the ratio of (Cp'-$d_{27}$)$_2$CeD to (Cp'-$d_{27}$)$_2$CeOPr in the $^2$H NMR spectrum was 1:1; the area ratio of the resonances corresponding to deuterium on the α- and γ-carbons of n-$Pr_2O$ was 2.5:1. The area

ratio of the proton resonances for the α-, β-, and γ-carbons of n-$Pr_2O$ in the $^1H$ NMR spectrum was 1:14:18.

**Cp'$_2$CeH and dibutyl ether (n-$Bu_2O$) in cyclohexane-$d_{12}$.**

Cp'$_2$CeH was dissolved in $C_6D_{12}$ in an NMR tube and a drop of n-$Bu_2O$ was added. The sample was heated at 60°C. After 6 days, resonances due to Cp'$_2$CeO-n-Bu had appeared in the $^1H$ NMR spectrum. The ratio of Cp'$_2$CeH to Cp'$_2$CeO-n-Bu was 24:1. After 30 days, the ratio was 4:1; after 99 days, 1:1.3; and after 147 days, 1:4. Gases from the headspace were condensed into a new tube containing $C_6D_6$ solvent cooled in a liquid nitrogen isopropanol bath. The $^1H$ NMR spectrum contained diamagnetic resonances at 1.22 and 0.85 ppm consistent with butane.

**(Cp'-$d_{27}$)$_2$CeD and n-$Bu_2O$ in $C_6D_6$**

Cp'$_2$CeH was dissolved in $C_6D_6$ and heated at 60°C for 4 days to perdeuterate the $CMe_3$ groups. The sample was taken to dryness and the solid residue was dissolved in fresh $C_6D_6$. The sample was heated for an additional 4 days, then taken to dryness, and the solid residue was dissolved in $C_6D_6$. The $^2H$ NMR spectrum contained $C(CD_3)_3$ resonances consistent with (Cp'-$d_{27}$)$_2$CeD. A drop of n-$Bu_2O$ was added, and the sample was heated at 60°C. After 1 day, a broad resonance at 3.21 ppm had appeared in the $^2H$ NMR spectrum indicating H-for-D exchange on the α-carbon of n-$Bu_2O$. The area ratio of the proton resonances on the α-, β-, γ-, δ-carbons had changed from 2:2:2:3 initially to 1:1.2:1.2:1.8. After 6 days, resonances due to (Cp'-$d_{27}$)$_2$CeOBu had appeared in the $^2H$ NMR spectrum; the ratio of (Cp'-$d_{27}$)$_2$CeD to (Cp'-$d_{27}$)$_2$CeOBu was 13:1. The ratio of the proton resonances on the α-, β-, γ-, δ-carbons of n-$Bu_2O$ in the $^1H$ NMR spectrum was 1:4:4:6. After 30 days, the ratio of (Cp'-$d_{27}$)$_2$CeD to (Cp'-$d_{27}$)$_2$CeOBu in the $^2H$ NMR spectrum was 5:1, and a multiplet had appeared at 0.82 ppm indicating H-for-D exchange on the δ-carbons of n-$Bu_2O$ as

well as on the α-carbons. The area ratio of the $^2$H NMR resonances for deuterium on the α- and δ-carbons of n-$Bu_2O$ was 30:1. The ratio of the proton resonances on the α-, β-, γ-, δ-carbons of n-$Bu_2O$ in the $^1$H NMR spectrum was 1:38:38:56. The $^{13}$C NMR spectrum contained a 1:3:5:3:1 pattern at 70.10 ppm ($J_{CD}$ = 21 Hz) for the α-carbons of n-$Bu_2O$, single resonances for the β- and γ- carbons, and a single resonance plus a 1:1:1 pattern ($J_{CD}$ = 19 Hz) centered 0.30 ppm upfield of the single resonance for the δ-carbon. After 147 days, resonances due to (Cp'-$d_{27}$)$_2$CeD were absent from the $^2$H NMR spectrum.

Gases from the sample headspace were condensed into a new tube containing $C_6D_6$ solvent cooled in a liquid nitrogen isopropanol bath. The $^1$H NMR spectrum contained a multiplet at 1.22 ppm and a triplet at 0.85 consistent with butane, but in a 1:1 area ratio. The $^2$H NMR spectrum contained a broad singlet at 1.28 ppm and a triplet at 0.76 in a 1:5 area ratio.

The solvent from the original sample was vacuum transferred into a fresh NMR tube. The $^1$H NMR spectrum contained resonances consistent with n-$Bu_2O$, but the resonance due to protons on the α-carbons had shifted upfield by 0.02 ppm, and each peak was split into a 1:1:1 pattern ($J_{HH}$ = 7 Hz, $J_{HD}$ = 1 Hz), consistent with α-CHD groups. The resonance for the protons on the β-carbon appeared as a triplet ($J_{HH}$ = 7 Hz), and the protons on the γ-carbon as a coincidental sextet (triplet of quartets, $J_{HH}$ = 7 Hz). The protons on the δ-carbon appeared as a triplet ($J_{HH}$ = 7 Hz) corresponding to δ-$CH_3$ groups, and another triplet with each peak split into a 1:1:1 pattern 0.018 ppm upfield corresponding to δ-$CH_2D$ groups. The area ratio of the α-, β-, γ-, and δ-carbon resonances was 1:45:45:59. The $^2$H NMR spectrum contained a triplet at 3.21 ($J_{HD}$ = 1 Hz) corresponding to the deuterons on the α-carbons and a multiplet at 0.83

corresponding to deuterons on the δ-carbons of n-$Bu_2O$; the area ratio of the two signals was 10:1. GCMS analysis of the solution showed the ratio of n-$Bu_2O$ -$d_2$, - $d_3$, $d_4$, $d_5$, and $d_6$ to be 3:3:32:7:1.

**Computational details**

The Stuttgart-Dresden-Bonn Relativistic large Effective Core Potential (RECP) was used to represent the inner shells of Ce.[19] The associated basis set[19] augmented by an f-polarization function ($\alpha$ = 1.000) was used to represent the valence orbitals.[20] The atoms C, O, and H were represented by an all-electron 6-31G(d,p) basis set.[21] Calculations were carried out at the DFT(B3PW91) level[22] with Gaussian 03.[23] The nature of the extrema (minimum or transition state) was established with analytical frequencies calculations and the intrinsic reaction coordinate (IRC) was followed to confirm that the transition states connect to reactants and products. The zero point energy (ZPE) and entropic contribution have been estimated within the harmonic potential approximation. The Gibbs free energy, G, was calculated at T = 298.15K and 1 atm.

**Acknowledgements**

This work was supported by the Director, Office of Science, Office of Basic Energy Sciences (OBES), of the U.S. Department of Energy (DOE) under Contract No. DE-AC02-05CH11231. A.Y thank the Computer Center, CCRT of the CEA for a generous donation of computation time. L.M. and O.E thank the CNRS and Minister of High Education and Research for funding, and A.Y. thanks the CEA for PhD fellowship. L.M. is a junior member of the Institut Universitaire de France.

**Electronic Supporting Information (ESI) available**

Coordinates, energies E and free energies G in a. u. of all calculated extrema.

**References**

1) E. L. Werkema, E. Messines, L. Perrin, L. Maron, O. Eisenstein and R. A. Andersen, *J. Am. Chem. Soc.,* 2005, **127**, 7781.

2) E. L. Werkema, R. A. Andersen, A. Yahia, L. Maron and O. Eisenstein, *Organometallics*, 2009, **28**, 3173.

3) P. L. Watson, *J. Chem. Soc. Chem. Commun.*, 1983, 276.

4) M. E. Thompson, S. M. Baxter, A. R. Bulls, B. J. Berger, M. C. Nolan, B. D. Santarsierio, W. P. Schaefer and J. E. Bercaw, *J. Am. Chem. Soc*, 1987, **109**, 203.

5) B. -J. Deelman, M. Booji, A. Meetsma, J. H. Teuben, H. Kooijman and A. L. Spek, *Organometallics,* 1995, **14**, 2306

6) W. J. Evans, T. A. Ulibarri and J. W. Ziller, *Organometallics*, 1991, **10**, 134.

7) E. L. Werkema, L. Maron, O. Eisenstein, and R. A. Andersen, *J. Am. Chem. Soc.* 2007, **129**, 2529. Correction *J. Am. Chem. Soc.* 2007, **129**, 6662.

8) E. L. Werkema, R. A. Andersen, L. Maron and O. Eisenstein, *Dalton Trans*., 2010 Advanced web publication.

9) S. Niu and M. B. Hall, *Chem. Rev.*, 2000, **100**, 353.

10) K. Ziegler and H.-G. Gellert, *Ann. Chem. Liebig.*, 1950, **567**, 185

11) A. Maercker and W. Demuth, *Angew. Chem. Int. Ed.*, 1973, **12**, 75. A. Maercker and W. Demuth, *Ann. Chem. Liebig.*, 1977, 1909. A. Maercher, *Angew. Chem. Int. Ed.*, 1987, **26**, 972. J. Clayden and S. A. Yasin, *New J. Chem.,* 2002, **26**, 191.

12) K. Tomooka, in *The Chemistry of Organolithium Compounds.* Part 2, Patai Series, The Chemistry of Functional Groups, Z. Rappoport and I. Marek Eds. Wiley 2004 pp 749-828. M. Braun, in *The Chemistry of Organolithium Compounds.* Part 2, Patai Series, The Chemistry of Functional Groups, Z. Rappoport and I. Marek Eds. Wiley 2004 pp 829-900.

13) V. H. Gessner and C. Strohmann, *J. Am. Chem. Soc.,* 2008, **130**, 14412.

14) C. A. Bradley, L. F. Veiros, D. Pun, E. Lobkovsky, I. Keresztes and P. J. Chirik, *J. Am. Chem. Soc.*, 2006, **128**, 16600.

15) W. A. Nugent, D. W. Ovenall and S. J. Holmes, *Organometallics,* 1983, **2**, 161. W. A. Nugent and R. M. Zubyk, *Inorg. Chem.,* 1986, **25**, 4604

16) L. Maron, E. L. Werkema, L. Perrin, O. Eisenstein and R. A. Andersen, *J. Am. Chem. Soc.,* 2005 **127**, 279.

17) A. Pierce, *Silylation of Organic Compounds: a Technique for Gas-Phase Analysis*, Pierce Chemical Company, Rockford, IL, 1968, p.18.

18) Okazaki, M.; Tobita, H.; Ogino, H., *Chem. Letters*, 1997, **26**, 437.

19) M. Dolg, H. Stoll, A. Savin and H. Preuß, *Theor. Chim. Acta,* 1989, **75**, 173. M. Dolg, H. Stoll and H. Preuß, *Theor. Chim. Acta,* 1993, **85**, 441.

20) L. Maron and O. Eisenstein, *J. Phys. Chem. A*, 2000, **104**, 7140.

21) P. C. Hariharan and J. A. Pople, *Theor. Chim. Acta,* 1973, **28**, 213.

22) J. J. P. Perdew and Y. Wang, *Phys. Rev. B*, 1992, **45,** 13244. A. D. Becke, *J. Chem. Phys.,* 1993, **98**, 5648. K. Burke, J. P. Perdew and Y. Wang, in "*Electronic Density Functional Theory: Recent Progress and New Directions"* J. F. Dobson, G. Vignale, and M. P. Das, Eds., **1998**, Plenum Press, New York.

23) M. J. Frisch, G. W. Trucks, H. B. Schlegel, G. E. Scuseria, M. A. Robb, J. R. Cheeseman, J. A. Montgomery, Jr., T. Vreven, K. N. Kudin, J. C. Burant, J. M. Millam, S. S. Iyengar, J. Tomasi, V. Barone, B. Mennucci, M. Cossi, G. Scalmani, N. Rega, G. A. Petersson, H. Nakatsuji, M. Hada, M. Ehara, K. Toyota, R. Fukuda, J. Hasegawa, M. Ishida, T. Nakajima, Y. Honda, O. Kitao, H. Nakai, M. Klene, X. Li, J. E. Knox, H. P. Hratchian, J. B. Cross, V. Bakken, C. Adamo, J. Jaramillo, R. Gomperts, R. E. Stratmann, O. Yazyev, A. J. Austin, R. Cammi, C. Pomelli, J. Ochterski, P. Y. Ayala, K. Morokuma, G. A. Voth, P. Salvador, J. J. Dannenberg, V. G. Zakrzewski, S. Dapprich, A. D. Daniels, M. C. Strain, O. Farkas, D. K. Malick, A. D. Rabuck, K. Raghavachari, J. B. Foresman, J. V. Ortiz, Q. Cui, A. G. Baboul, S. Clifford, J. Cioslowski, B. B. Stefanov, G. Liu, A. Liashenko, P. Piskorz, I. Komaromi, R. L. Martin, D. J. Fox, T. Keith, M. A. Al-Laham, C. Y. Peng, A.

Nanayakkara, M. Challacombe, P. M. W. Gill, B. G. Johnson, W. Chen, M. W. Wong, C. Gonzalez and J. A. Pople, GAUSSIAN 03 (Revision C.02), Gaussian, Inc., Wallingford, CT, 2004.

**TOC and abstract text**

The mechanism of the C-O bond cleavage in ethers is shown with reactants and observed products circled in green.